



HAL
open science

Secretion of Hepatitis C Virus Replication Intermediates Reduces Activation of Toll-Like Receptor 3 in Hepatocytes

Oliver Grünvogel, Ombretta Colasanti, Ji-Young Lee, Volker Klöss, Sandrine Belouzard, Anna Reustle, Katharina Esser-Nobis, Jasper Hesebeck-Brinckmann, Pascal Mutz, Katrin Hoffmann, et al.

► To cite this version:

Oliver Grünvogel, Ombretta Colasanti, Ji-Young Lee, Volker Klöss, Sandrine Belouzard, et al.. Secretion of Hepatitis C Virus Replication Intermediates Reduces Activation of Toll-Like Receptor 3 in Hepatocytes. *Gastroenterology*, 2018, 154 (8), pp.2237-2251.e16. 10.1053/j.gastro.2018.03.020 . hal-02112499

HAL Id: hal-02112499

<https://hal.science/hal-02112499>

Submitted on 26 Apr 2019

HAL is a multi-disciplinary open access archive for the deposit and dissemination of scientific research documents, whether they are published or not. The documents may come from teaching and research institutions in France or abroad, or from public or private research centers.

L'archive ouverte pluridisciplinaire **HAL**, est destinée au dépôt et à la diffusion de documents scientifiques de niveau recherche, publiés ou non, émanant des établissements d'enseignement et de recherche français ou étrangers, des laboratoires publics ou privés.



Distributed under a Creative Commons Attribution 4.0 International License

1 **SECRETION OF HEPATITIS C VIRUS REPLICATION INTERMEDIATES DAMPENS TOLL-LIKE**
2 **RECEPTOR 3 ACTIVATION IN HEPATOCYTES**

3 **Oliver Grünvogel^a, Ombretta Colasanti^a, Ji-Young Lee^a, Volker Klöss^b, Sandrine Belouzard^c, Anna**
4 **Reustle^{a*}, Katharina Esser-Nobis^{a#}, Jasper Hesebeck-Brinckmann^a, Pascal Mutz^{a,i}, Katrin Hoffmann^d,**
5 **Arianeb Mehrabi^d, Ronald Koschny^e, Florian W. R. Vondran^{f,g}, Daniel Gotthardt^{e§}, Paul Schnitzler^h,**
6 **Christoph Neumann-Haefelinⁱ, Robert Thimmeⁱ, Marco Binder^j, Ralf Bartenschlager^{a,j}, Jean**
7 **Dubuisson^c, Alexander H. Dalpke^b, Volker Lohmann^a**

8 Corresponding Author: Dr. Volker Lohmann, Department of Infectious Diseases, Molecular Virology,
9 University of Heidelberg, Im Neuenheimer Feld 345, 69120 Heidelberg, Germany.

10 volker.lohmann@med.uni-heidelberg.de

11 **Affiliations:** Department of Infectious Diseases, Molecular Virology, University of Heidelberg,
12 Heidelberg, Germany^a; Department of Infectious Diseases, Medical Microbiology and Hygiene,
13 University Hospital Heidelberg, Heidelberg, Germany^b; Univ. Lille, CNRS, Inserm, CHU Lille, Institut
14 Pasteur de Lille, U1019 - UMR 8204 - CIIL- Centre d'Infection et d'Immunité de Lille, F-59000 Lille,
15 France^c; Department of General-, Visceral- and Transplantation Surgery, University Hospital
16 Heidelberg, Heidelberg, Germany^d; Department of Gastroenterology, Infectious Diseases and
17 Intoxication, University Hospital Heidelberg, Heidelberg, Germany^e, Regenerative Medicine and
18 Experimental Surgery (ReMediES), Department of General, Visceral and Transplant Surgery,
19 Hannover Medical School, Hannover, Germany^f; German Center for Infection Research (DZIF),
20 partner site Hannover-Braunschweig, Hannover, Germany^g; Department of Infectious Diseases,
21 Virology, University of Heidelberg, Heidelberg, Germany^h; Department of Medicine II, Medical
22 Center - University of Freiburg, Faculty of Medicine, University of Freiburgⁱ. Division of Virus-
23 Associated Carcinogenesis (F170), German Cancer Research Center (DKFZ), Heidelberg, Germany^j.

24 Present address: Dr. Margarete Fischer-Bosch-Institute of Clinical Pharmacology, Stuttgart,
25 Germany*; Department of Immunology, University of Washington, Seattle, Washington, USA#;
26 [Mediteo GmbH, Heidelberg, Germany](#)[§]

27 **Grant Support:** This project was supported by grants from the Deutsche Forschungsgemeinschaft
28 (TRR179-TP17, FOR1202-TP3 to V.L.; TRR179-TP9, FOR1202-TP1 to R.B., TRR179-TP1 to R.T. and
29 TRR179-TP2 to C.N.-H.). This work was supported by a grant from the Excellence Cluster Cellular
30 Networks of University of Heidelberg (to A.D. and V.L.)

31 **Disclosures:** All authors declare no conflicts of interest.

32 **Short Title:** HCV dsRNA secretion and TLR3 activation

33 **Abbreviations:** DMV, double-membrane vesicle; dsRNA, double-stranded RNA; EVs, extracellular
34 vesicles; HCV, Hepatitis C virus; HCVcc, cell culture derived HCV; i.c., intracellular; MAVS,
35 mitochondrial antiviral signaling protein; MDA5, melanoma differentiation-associated protein 5;
36 MMV, multi-membrane vesicle; MVB, multivesicular body; PRR, pattern recognition receptor; RIG-I,
37 retinoic-acid inducible gene I; TLR3, toll-like receptor 3

38 **Author Contributions:** O.G. conceived and carried out experiments, interpreted the results and
39 wrote the manuscript. J.Y.L. performed CLEM experiments. O.C., V.K., A.R., J.H.B. and K.E.N.
40 performed some of the experiments. S.B. and J.D. performed experiments with polarized
41 hepatocytes. P.M., K.H., A.M., R.K. and F.W.R.V. provided PHH. D.G., P.S., C.N.H. and R.T. provided
42 patient serum samples. M.B. provided critical reagents. R.B. and A.D. contributed to the concept of
43 the work and the interpretation of results. V.L. designed the concept of the project, interpreted the
44 results and wrote the manuscript. All authors contributed to the writing of the manuscript.

45 **Word Count: 7232**

46 **ABSTRACT**

47 **Background and aims**

48 Hepatitis C virus (HCV) infections most often result in chronic outcomes, although the virus
49 constantly produces replication intermediates, in particular double-stranded RNA (dsRNA),
50 representing potent inducers of innate immunity. We aimed to characterize the fate of HCV dsRNA
51 in hepatocyte cultures to identify mechanisms contributing to viral persistence in presence of an
52 active innate immune response.

53 **Methods**

54 Various hepatocyte based cell culture models for HCV were analyzed for induction of innate
55 immunity, secretion of viral positive/negative strand RNA and viral replication using different
56 quantification methods and microscopy techniques. Expression of pattern recognition receptors was
57 reconstituted in hepatoma cells by lentiviral transduction.

58 **Results**

59 HCV infected cells secrete substantial amounts of viral positive and negative strand RNA in
60 extracellular vesicles (EVs), towards the apical and basolateral domain of hepatocytes. Secretion of
61 negative strand RNA was independent from virus production and viral RNA secreted in EVs
62 contained higher relative amounts of negative strands, indicating that mainly viral dsRNA is released.
63 A substantial part of viral replication complexes and dsRNA was found in the endosomal
64 compartment/multivesicular bodies, suggesting that secretion of HCV replication intermediates is
65 mediated by the exosomal pathway. Block of vesicle release in HCV-positive cells increased
66 intracellular dsRNA levels and led to an increased activation of toll-like receptor 3 (TLR3), inhibiting
67 HCV replication.

68 **Conclusion**

69 Our results demonstrate that part of the HCV dsRNA intermediates are released from infected cells
70 in EVs attenuating activation of TLR3. This mechanism represents a novel strategy to dampen
71 intracellular innate immune responses, potentially contributing to the establishment of persistence.

72

73 **Keywords:** exosomes, escape

74

75 INTRODUCTION

76 Hepatitis C virus (HCV) presents a global health problem, as it persistently infects about 1 % of the
77 world's population, and about 75% of all HCV infections will progress to a chronic stage¹. HCV is a
78 positive-strand RNA virus of the *flaviviridae* family, and primarily replicates in human hepatocytes.
79 Upon infection, viral proteins induce formation of membranous replication organelles, consisting
80 primarily of typical double membrane vesicles (DMVs), the presumed site of viral RNA replication,
81 and multi-membrane vesicles (MMVs)². HCV forms a double-stranded RNA (dsRNA) replication
82 intermediate during its replication process, and persistently HCV-infected cells constantly produce
83 new DMVs³. However, only about 30% of replication complexes are considered to actively support
84 RNA replication in HCV-infected cells⁴. The fate of inactive replication complexes remains unknown.

85 Viral dsRNA in general is a major pathogen associated molecular pattern (PAMP) inducing innate
86 immune responses. Hepatocytes express several pattern recognition receptors (PRRs) for detection
87 of dsRNA, including the cytoplasmic sensors retinoic-acid inducible gene I (RIG-I) and melanoma
88 differentiation-associated protein 5 (MDA5)⁵, and the endosomal toll-like receptor 3 (TLR3)⁶.

89 However, HCV counteracts the activation of these sensors by proteolytic cleavage of the
90 mitochondrial antiviral signaling protein (MAVS), efficiently inhibiting the production of interferon
91 (IFN) and interferon-stimulated genes (ISGs)⁷. In the TLR3 signaling pathway, the HCV protease
92 NS3/4A cleaves the adaptor TIR domain-containing adapter molecule 1 (TRIF)⁸, yet the efficiency of
93 inhibiting TLR3-induced upregulation of IFNs and ISGs by this mechanism is still discussed
94 controversially^{6,9}.

95 HCV-infected cells not only secrete regular infectious virions, but also infectious genomic RNA in
96 exosomes, which are a subpopulation of extracellular vesicles (EVs)^{10,11}. These vesicles with a
97 diameter of 50-150 nm are formed by budding into the outer limiting membrane of the
98 multivesicular body (MVB), a sorting vehicle of late endosomal origin¹². The MVB content can then
99 be degraded by fusion with a lysosome¹³, a process in which the content could come into contact

100 with endo-lysosomal TLR3. On the other hand, if the MVB fuses with the plasma membrane, the
101 intraluminal vesicles are released to the exterior as exosomes, transporting proteins, mRNAs and
102 miRNAs to mediate cell-cell communication¹⁴. The release of HCV particles is linked to the exosomal
103 release pathway^{15,16}, but HCV RNA is also released in exosomes in the absence of viral structural
104 proteins^{10,11}. HCV RNA released in exosomes can have a dual function, as it can activate innate
105 immune cells, such as plasmacytoid dendritic cells (pDCs), to trigger production of antiviral IFN- α ¹⁰ or
106 it can propagate the infection to naïve cells, while being shielded from neutralization^{11,17}.

107 Here, we determined the contribution of the late endosomal / exosomal RNA release pathway to the
108 fate of HCV replication complexes and replication intermediates, and evaluated the potential impact
109 on the activation of PRRs in HCV-infected cells. We found that dsRNA indeed was secreted from
110 HCV-positive cells. Blocking of dsRNA release strongly increased the activation of TLR3 and its
111 antiviral effects on HCV replication. Secretion of dsRNA therefore represents a novel immune
112 evasion mechanism employed by HCV to dampen the activation of innate immune responses within
113 the infected cell.

114 **MATERIAL AND METHODS**

115 Unless specified below, detailed information about used materials and methods can be found in the
116 supplementary materials and methods section.

117 **Cell Culture**

118 All cell lines were cultured in Dulbecco's Modified Eagle Medium (DMEM; Life Technologies,
119 Darmstadt, Germany) supplemented with 10% fetal bovine serum, non-essential amino acids (Life
120 Technologies, Darmstadt, Germany), 100 U/ml penicillin and 100 ng/ml streptomycin (Life
121 Technologies) and cultivated at 37°C and 5% CO₂. Huh7-Lunet cells and Huh7-Lunet-CD81^{high} cells
122 have been described before¹⁸, as well as the Con1 subgenomic replicon clone 9-13 (gt 1b), cell lines
123 with persistent reporter replicons of genotype 2a (LucubineoJFH1)¹⁹ and HAV replicon cell lines²⁰.

124 Cells were kept under selection pressure by addition of 1mg/ml G418 (Geneticin, Life Technologies),

125 1µg/ml puromycin (Sigma-Aldrich, Steinheim, Germany) or 5µg/ml blasticidin (Sigma-Aldrich). Clones
126 15 and 1SC3 of the HepG2-CD81 cell line were described recently²¹, and were grown on semi-
127 permeable support (Corning) in William's medium supplemented with 2mM glutamax, 10 ng/ml
128 gentamicin and 1% DMSO to induce cell polarity development.

129 **Primary Human Hepatocytes (PHH)**

130 Liver samples were obtained either after partial liver resection for medical reasons or from organ
131 donors when the liver was considered unsuitable for transplantation. Primary human hepatocytes
132 (PHH) were isolated as described before^{22,23}. Tissue donors gave written informed consent for the
133 experimental use of their specimens. The protocol was approved by the ethics commission of
134 Hannover Medical School (#252-2008). Ethical approval further is covered with reference number #
135 S-161/2007. Isolated PHH were cultured in Williams E medium (Life Technologies), supplemented
136 with 10% FCS (Seromed, heat inactivated), 50 U/ml penicillin / 50 µg/ml streptomycin antibiotics, 50
137 µM hydrocortisone and 5 µg/ml insulin (SAFC, Sigma Aldrich), and incubated at 37° C and 5% CO₂.

138 **Exosome Isolation**

139 For Extracellular vesicle (EV)-isolation, cells were grown in EV-depleted medium, which was
140 generated by ultracentrifugation of fetal bovine serum at 110,000 g for 16h at 4°C. EVs were isolated
141 using Exo-spin Exosome Purification Kit (Cell Guidance Systems, Cambridge, UK) according to
142 manufacturer's protocol, with the addition of a filtration step with 0.22 µm filters after the final pre-
143 clearing centrifugation.

144 **Statistical analysis**

145 Independent biological replicates are denoted with n-numbers. To test for significance, two-tailed
146 paired t-test or Welch's test was performed using GraphPad Prism 5 software (GraphPad Software,
147 La Jolla, CA, USA). * p<0.05; ** p<0.01; *** p<0.001.

148 RESULTS

149 HCV RNA secreted in extracellular vesicles is enriched for negative strand

150 HCV genomic RNA has been described to be secreted in exosomes^{10,11}. We therefore hypothesized
151 that these EVs might also contain HCV negative strand RNA, indicative for the secretion of viral
152 replication intermediates. We isolated EVs from HCV infected Huh7-Lunet CD81high cells¹⁸ (strain
153 Jc1, Fig. 1A), which likely also contained co-purified infectious virus due to similar biophysical
154 properties¹⁰ and investigated the composition of HCV RNA in these vesicles relative to intracellular
155 viral RNA by use of a strand-specific RT-qPCR assay (Fig. S1A,B). Since negative strand RNA was used
156 as a quantitative marker for dsRNA, we ensured that our assay reached a sensitivity of minus strand
157 detection comparable to a previously published protocol (²⁴, Fig. S1C). We found substantial amounts
158 of negative strands in the EV fraction of infected cells, with a far lower relative ratio of positive to
159 negative strands than intracellularly (3.8 vs 29.8, respectively (Fig. 1B)). Secretion of negative strand
160 RNA started at about 24h after infection and showed similar kinetics as the secretion of positive
161 strand RNA (Fig. 1C). We further analyzed HCV infected primary human hepatocytes (PHH) to
162 confirm the secretion of viral replication intermediates in a more physiological cell culture system.
163 Amounts of secreted RNA were lower in PHH than in HCV-infected Huh-7 cells and varied between
164 donors, which is most likely due to lower replication of HCV, because of the strong counteraction by
165 innate immune responses in PHH²⁵. However, negative strand RNA secretion in EVs again
166 recapitulated secretion kinetics of positive strand (Fig. 1D, S1D, E). Importantly, also in PHH relative
167 amounts of negative strand HCV RNA in EVs were strongly increased compared to intracellular levels
168 (Fig. 1E). We next used cell lines harboring persistent subgenomic HCV replicons, lacking the coding
169 region of structural proteins (Fig. 1A), to assess the impact of virion production on secretion of
170 negative strand RNA. Cells harboring replicons of different genotypes secreted similar amounts of
171 negative strand RNA in EVs as HCV infected cells, but lower levels of positive strands, likely due to
172 the absence of virions (Fig. 1F,G), which co-purify with EVs due to similar biophysical properties¹⁰.
173 Therefore, negative strand RNA was clearly enriched in EVs as compared to levels in HCV-infected

174 and replicon cells (Fig. 1H). We further assessed the kinetics of RNA release from replicon cells,
175 which reached steady state levels 15 min. after medium exchange (Fig. S1F). This result suggested
176 that, albeit steady state RNA levels are moderate compared to intracellular viral RNA, a higher
177 amount of negative strand RNA might be secreted due to rapid secretion kinetics and high turnover.
178 Overall these data argued for enrichment and secretion of substantial amounts of dsRNA in EVs.
179 Since subgenomic replicons allowed the analysis of HCV RNA secretion independent from virion
180 production we mainly used this model throughout this study. We first verified that secreted HCV
181 RNA was protected by membranes as deduced from RNase resistance in the absence of detergent
182 (Fig. S2A). We further verified that the exosomal fraction contained the marker CD63, as well as
183 small amounts of NS5A (Fig. S2B), in line with a recent study²⁶, supporting the hypothesis that the
184 secreted viral RNA might be contained in previous replication vesicles. The secretion of HCV RNA
185 could be decreased by GW4869, an inhibitor of neutral sphingomyelinase 2, blocking exosome
186 release as previously reported^{10,27}, as well as by knocking down Rab27a, an important host factor in
187 the release pathway of exosomes (Fig. S2C-D)²⁸, with the combination of GW4869 and siRNA
188 showing increased efficiency, probably due to targeting of different steps involved in the exosome
189 release pathway. Knockdown of Rab27a was specific, as reconstitution of RAb27a expression
190 rescued HCV RNA release (Fig. S2E). In addition, Rab27a KD had no detrimental effects on cell
191 viability (Fig. S2F). In contrast to HCV, viral RNA was almost undetectable in extracellular vesicles
192 purified from the supernatant of HAV replicon cells (Fig. S2G), suggesting that secretion of viral
193 replication intermediates in EVs is not common for all hepatotropic RNA viruses.

194 Altogether, these data suggested that HCV replication intermediates are secreted in EVs/exosomes,
195 as previously shown for positive strand RNA¹⁰. Moreover, HCV negative strand RNA was highly
196 enriched in the secreted fraction as compared to intracellular levels.

197 **HCV replication intermediates are detected in the late endosomal compartment**

198 We next analyzed the intracellular localization of viral replication organelles in replicon cells. Since
199 secretion of viral RNA in EVs was blocked by inhibitors of exosome release we particularly focused
200 on detection of viral replication organelles and dsRNA in MVBs and endosomal compartments.

201 We used a replicon harboring an insertion of mCherry in nonstructural protein (NS)5A (Fig. 2A), and
202 implemented correlative light and electron microscopy to assess the ultrastructure of NS5A-positive
203 regions (Fig. 2B,C). About 25% of NS5A positive regions showed no distinct substructures (Fig. 2D,
204 other). About 35% of NS5A-mCherry signals were associated with cytoplasmic regions representing
205 the viral replication organelle, as judged by the presence of DMVs and MMVs (Fig. 2C, area 2; Fig.
206 2D, DMVs). In addition, NS5A signal could be detected at lipid droplets (LD), the endoplasmatic
207 reticulum (ER), and the mitochondria (Fig. 2D, Fig. S3). Surprisingly, more than 20% of all NS5A
208 positive regions per cell were in fact multivesicular bodies (MVBs) or lysosomes (Fig. 2C, area 3; Fig.
209 2D). Most of these NS5A-positive MVBs also contained DMVs and MMVs (Fig. 2E, Fig. S3). This
210 observation was in line with our hypothesis that secreted HCV replication intermediates originate
211 from the MVB, as previously reported for genomic RNA secreted in exosomes¹⁰. We next assessed
212 the colocalization of dsRNA with markers of the MVB/lysosomes using immunofluorescence-based
213 staining, confocal microscopy and 3D reconstruction. Indeed, dsRNA was detected in CD63-positive
214 compartments and in association with the late endosomal/lysosomal marker Lamp1, adding up to
215 about 20% and 15% of all dsRNA signals in HCV-positive cells, respectively (Fig. 2F-H).

216 To further support the mechanistic link between secretion of HCV replication intermediates and the
217 late endosome/MVB, we blocked the exosomal release pathway by knockdown of Rab27a. While
218 release of HCV RNA in EVs was decreased in Rab27a-KD cells (Fig. 3A), intracellular dsRNA levels
219 were significantly increased (Fig. 3C), which was confirmed by strand-specific RT-qPCR, using
220 negative strand as a marker of dsRNA (Fig. S4). More specifically, knockdown of Rab27a increased
221 the dsRNA amounts associated with CD63+ exosome release compartments and Lamp1+ lysosomal

222 compartments (Fig. 3E, G). In contrast, when lysosomal acidification was inhibited by Bafilomycin A
223 (BafA), significantly higher amounts of HCV RNA were secreted (Fig. 3B), while the number of
224 intracellular dsRNA positive signals decreased (Fig. 3D). Consequently, also a lower number of
225 dsRNA signals was found associated with CD63+ and Lamp1+ compartments.

226 (Fig. 3F, H).

227 Altogether, our data suggested that HCV dsRNA, engulfed in vesicular structures, entered the
228 endosomal pathway, from where it was either secreted in EVs or entered the lysosomal
229 compartment.

230 **TLR3 can be activated within HCV-positive cells**

231 As dsRNA is a strong inducer of innate immune responses, we next studied the impact of dsRNA
232 release on the activation of intracellular PRRs. Hepatocytes constitutively express the cytosolic
233 dsRNA sensors RIG-I and MDA5, as well as the endosomal dsRNA sensor TLR3⁸. Indeed, ISG
234 expression was strongly induced in PHH upon transfection of poly(I:C) and by delivery of poly(I:C) to
235 the supernatant, thus only accessible for uptake in endo-lysosomes and exclusively activating TLR3
236 (Fig. 4A, PHH). In contrast, Huh7-Lunet cells barely responded to either of these stimuli (Fig. 4A,
237 empty), indicating low expression of the PRRs. We therefore reconstituted expression of individual
238 dsRNA sensor, leading to rescue of dsRNA recognition upon poly(I:C) stimulation (Fig. 4A, S5A). We
239 chose IFIT1 mRNA levels as a robust measure of ISG responses induced by all PRRs⁵, whereas IFN β
240 mRNA was not detectable in Huh7 cells expressing TLR3 (Fig. S5C) and not induced in PHH by
241 addition of poly(I:C) to the supernatant (Fig. S5D), as reported⁹.

242 We next assessed ISG induction by each PRR and its corresponding impact on HCV replication by
243 transfection of a subgenomic HCV reporter replicon (Fig. 4B). Expression of RIG-I resulted in an early
244 and transient induction of IFIT1 mRNA levels (Fig. 4C), likely by the incoming RNA and blocked by
245 cleavage of MAVS at later time points⁷. Expression of MDA5 did not result in induction of ISG
246 response and neither RIG-I nor MDA5 expression had any significant impact on HCV replication (Fig.

247 4D). In contrast, presence of TLR3 induced strong expression of IFIT1 mRNA, starting 48 h after
248 transfection of the replicon (Fig. 4C), correlating with impaired viral replication, with a 24 h delay
249 (Fig. 4D). TLR3 expression was similar to PHH (Fig. S5B), indicating that TLR3 activation was likely not
250 an artefact of overexpression. The induction of ISG responses and its negative impact on HCV
251 replication upon TLR3 activation was further confirmed in cell lines containing a persistent reporter
252 replicon (Fig. 4E). Transient transduction with a lentiviral vector expressing TLR3 induced a strong
253 ISG response and decreased HCV replication also in this case (Fig. 4F,G). In contrast, HCV infection
254 did result in a delayed, slightly less pronounced activation of TLR3⁵, which did not result in a clear
255 reduction of HCV replication in the time frame of the experiment (Fig. S6), either due to differences
256 in the kinetics of dsRNA production and/or by the increased levels of secreted dsRNA found upon
257 infection, dampening TLR3 response.

258 TLR3 is typically activated by endocytic uptake of extracellular dsRNA and it has been shown that
259 HCV can cause TLR3 activation in uninfected cells by extracellular transfer of dsRNA²⁹. We performed
260 co-culture experiments to investigate the contribution of secreted dsRNA to trans-activation of
261 neighboring cells versus the induction of TLR3 upon intracellular transfer of replication
262 intermediates. We either transfected subgenomic HCV replicons into Huh7-Lunet-TLR3 cells and co-
263 cultured them with the same cell type lacking TLR3, resulting in a strong induction of IFIT1 mRNA
264 expression (Fig. 4H, bottom). In contrast, the same replicons transfected into Huh7-Lunet cells
265 lacking TLR3 and co-cultured with Huh7-Lunet-TLR3 only caused minimal IFIT1 induction (Fig. 4H,
266 top). This result showed that TLR3 is activated mostly within HCV-positive cells and that transfer of
267 dsRNA played a minor role.

268 In summary, TLR3 elicits antiviral ISG responses in HCV-positive cells, despite the presence of viral
269 protease. The activation of TLR3 did not depend on extracellular but on intracellular transfer of
270 dsRNA.

271 **HCV dsRNA secretion decreases activation of TLR3**

272 TLR3 resides in the late endosome, in which HCV dsRNA replication intermediates were detected.

273 Therefore, we investigated the effect of blocking dsRNA release in EVs on the activation of TLR3.

274 Huh7-Lunet-TLR3 or empty control cells were transfected with HCV reporter replicon RNA and

275 release of EVs was inhibited by knockdown of siRab27a (Fig. S7A) and/or treatment with GW4869,

276 which in combination was most efficient in preventing HCV RNA secretion (Fig. S2C). GW4869

277 treatment itself had no impact on poly(I:C)-induced TLR3 activation (Fig. S7B), and showed no

278 detrimental effects on cell viability (Fig. S7C, D).

279 Neither treatment affected ISG induction or HCV replication in control cells (Fig. 5A, C), or impacted

280 HCV replication in cells expressing RIG-I or MDA5 (Fig. S8). In addition, replication of DENV reporter

281 replicons was not influenced by blocking EV secretion in any of the dsRNA-sensor-expressing cell

282 lines, while HAV replication was inhibited by Rab27a knockdown independently of PRR expression

283 (Fig. S9). In contrast, siRab27a and GW4869 treatment both lead to higher ISG induction at earlier

284 time points in TLR3-expressing cells upon HCV replication than the non-treated controls (Fig. 5B).

285 Consequently, the increased induction of ISGs resulted in a significant decrease in HCV replication

286 upon blocking of EV secretion (Fig. 5D). This result indicated that secretion of HCV dsRNA indeed

287 reduced the TLR3 response induced by HCV replication, albeit we cannot formally rule out the

288 possibility that other exosomal content might additionally regulate TLR3 response. Increased

289 induction of ISG expression was also observed in HCVcc-infected cells expressing TLR3 upon EV

290 release inhibitor treatment (Fig. 5E,F). However, the release of infectious virus is at least partially

291 dependent on the exosome release pathway^{15,16}, therefore Rab27a knockdown and GW4869

292 treatment resulted in decreased secretion of infectious virus and slightly increased intracellular RNA

293 levels in presence and absence of TLR3, precluding an unequivocal interpretation of the replication

294 data (Fig. S10).

295 In summary, release of HCV dsRNA in EVs decreased the activation of TLR3 in HCV-positive cells.
296 Therefore, secretion of dsRNA represents an escape mechanism dampening cell intrinsic innate
297 immune responses.

298 **HCV negative strand RNA is secreted at both sides of polarized hepatocytes and is lowly abundant**
299 **in serum of chronically-infected patients**

300 Our work so far demonstrated that secretion of dsRNA by HCV infected cells weakens intracellular
301 TLR3 responses, thus facilitating viral replication. However, previous work has shown that secreted
302 HCV positive strand RNA might activate pDCs to produce IFN, counteracting HCV replication¹⁰. Since
303 hepatocytes are highly polarized cells, EVs are secreted not only at the basolateral, sinusoidal side,
304 but also at the apical side, into bile canaliculi. Therefore, we wondered whether all HCV negative
305 strand RNA indeed is secreted to the basolateral surface, potentially capable of activating pDCs, or at
306 least in part to the apical side, thereby avoiding activation of innate immune responses. We
307 therefore employed a cell culture system based on HepG2 cell clones with polarization capabilities.
308 These recently described cell clones are the so far only cell lines permissive for HCV infection that
309 can be polarized on transwell inserts to form an intact apical and basolateral compartment²¹. Only
310 this experimental setting allowed collecting and analyzing media from both compartments
311 separately. After infection with HCV, these cells secrete infectious HCV particles as well as EVs on
312 both their apical and their basolateral side. We isolated RNA from the apical and basolateral
313 supernatants from two independent cell clones infected with HCVcc and analyzed their HCV RNA
314 composition. Both cell clones secreted the majority of HCV RNA at the basolateral side (Fig. 6A, 6C).
315 This correlated with the preferential secretion of infectious HCV particles at the basolateral side²¹.
316 However, HCV RNA from apical supernatants was enriched for negative strand RNA in both clones
317 (Fig. 6B, D), suggesting a substantial secretion of dsRNA at the apical side.

318 Finally, we analyzed the abundance of positive and negative strand RNA in EVs purified from the
319 serum of 5 patients with chronic HCV infection. Interestingly, we could detect significant amounts of

320 negative strand RNA in all sera, albeit at far lower and highly variable ratios compared to cell culture
321 supernatants (Fig. 6E), indicating that serum predominantly contains infectious virus and that the
322 majority of dsRNA secreted in EVs does not reach the systemic circulation. Since a previous study has
323 observed increased levels of dsRNA in the liver of chronic HCV patients depending on their IL28B
324 genotype²⁴, it will be interesting to analyze in future studies whether this correlates with negative
325 strand levels in the serum.

326 In summary, polarized HepG2 cells infected with HCV secreted negative strand RNA partly at their
327 apical side, away from systemic circulation. In line with these results, we could detect negative
328 strand viral RNA in the sera of HCV infected patients, but to a far lower extent than in cell culture.

329 In conclusion, our results demonstrate that HCV dsRNA enters the endosomal compartment, where
330 it is either released in EVs, or activates TLR3. Release of dsRNA replication intermediates attenuates
331 TLR3 responses, thereby representing a mechanism to avoid excessive activation of cell intrinsic
332 innate immunity. In addition, dsRNA replication intermediates are partly secreted at the apical side
333 of polarized hepatocytes, away from access to systemic circulation and detection by professional
334 immune cells. Our findings add another mechanism to the repertoire of immune evasion strategies
335 employed by HCV.

336 **DISCUSSION**

337 This study shows that viral replication vesicles containing dsRNA enter the endosomal pathway and
338 are either secreted in EVs via the MVB or transported into lysosomes, activating TLR3 (Fig. 7A).

339 Blocking EV secretion by the MVB pathway strongly increases TLR3 activation, mounting a stronger
340 antiviral response, suggesting that secretion of dsRNA and lysosomal degradation are governed by
341 the same mechanism (Fig. 7B). Therefore, secretion of dsRNA replication intermediates in EVs
342 alleviates induction of TLR3 responses in HCV-infected hepatocytes, representing a novel viral
343 immune escape mechanism.

344 Our results demonstrate that substantial amounts of HCV negative strand are secreted in
345 extracellular vesicles, likely exosomes, by HCV infected cells. The interpretation that these negative
346 strands indeed are dsRNA replication intermediates engulfed in replication vesicles is supported by
347 the high ratio of negative to positive strand RNA found in the secreted fraction and presence of
348 NS5A positive DMVs/MMVs, as well as dsRNA in late endosomes/MVBs. Secretion of these viral
349 replication vesicles is independent from presence of structural proteins; however, egress of a
350 subfraction of infectious virions also follows this route^{15,16}. A mechanistic link between both
351 processes is suggested by an increased efficiency of viral positive strand RNA release in exosomes in
352 the context of full viral replication³⁰, which was also found in our analysis of negative strand RNA
353 secretion. The detailed mechanism underlying transport to the endosome and secretion of viral
354 replication intermediates in EVs, as well as infectious virus, remains to be determined. Previous
355 studies suggested involvement of the ESCRT complex^{10,31}. Alternatively, autophagy has been
356 suggested to play a role in generation of viral replication complexes as well as release of infectious
357 HCV virions^{16,32}. We can furthermore not rule out that replication vesicles are directly formed at the
358 MVB.

359 HCV is known to activate TLR3, which is expressed constitutively in hepatocytes⁶. Conversely, HCV is
360 reported to cleave the TLR3 adaptor TRIF to blunt this pathway⁸, whereas other reports claim that
361 the TLR3 pathway is not efficiently shut off during HCV replication^{6,9}. Our data strongly support the
362 latter studies, since selected replicon cells, by definition all containing replicating viral RNA and
363 expressing the NS3/4A protease, remained fully susceptible to TLR3 signaling. Our results further
364 suggest that TLR3 is mostly activated upon intracellular delivery of viral replication vesicles to the
365 endosomal/lysosomal compartment within the HCV-replicating cell itself, and not by transfer of
366 naked RNA to neighbouring cells²⁹, although we cannot formally rule out, that TLR3 is activated by
367 autocrine secretion and re-entry of viral dsRNA. Overall TLR3 seems as important in detecting
368 intracellular HCV RNA as the cytosolic sensors RIG-I and MDA5, since we only found a moderate,
369 transient RIG-I activation at early time points, compared to a sustained TLR3 response starting at 48h

370 after infection. For several reasons, it is currently difficult to evaluate to which extent TLR3 indeed
371 contributes to high ISG expression in hepatocytes even in chronic patients³³⁻³⁵. First, ISG responses
372 mounted by cytosolic PRRs, TLR3 and paracrine Type I or Type III IFNs are very similar and hard to
373 differentiate⁹. Second, in PHH, early secretion of IFNs, likely induced by RIG-I activation, masks
374 possible late TLR3 responses. In future studies, the contribution of TLR3 to intrahepatic ISG
375 responses against HCV might be addressed upon availability of fully immunocompetent animal
376 models by selective knockdown/knockout of PRRs.

377 Secretion of HCV RNA in exosomes/EVs has been described in previous studies as an antiviral sensing
378 process activating innate immune responses in DCs, NK cells and monocytes^{10,36,37}, inducing
379 interferon responses and inhibiting viral replication. However, activation requires close cell to cell
380 contact. In addition, several studies indicate that elevated ISG expression in the liver of chronic HCV
381 patients is found primarily in HCV positive hepatocytes and their surrounding cells, suggesting that
382 intracellular and not immune cell-derived innate immune responses might substantially contribute
383 to ISG induction^{34,38,39}. Our work now shows that mainly double stranded HCV RNA is secreted in EVs,
384 dampening intracellular detection by TLR3. We further demonstrate significant secretion of dsRNA,
385 but not virions, into the apical compartment, towards the bile duct, using a new model of polarized
386 hepatocytes in transwells²¹. This result is in line with previous studies detecting HCV RNA in bile⁴⁰
387 and stool⁴¹ of chronic HCV patients and strongly argues for an escape mechanism evolved by HCV,
388 reducing antiviral innate immune responses in infected cells and preventing detection of secreted
389 RNA by the cellular innate immune response. Interestingly, we found no evidence for substantial
390 secretion of viral RNA in case of HAV and Dengue virus replicon cells, nor did blocking of exosome
391 release inhibit viral replication, as was the case for HCV. Since HAV and Dengue virus cause only
392 acute infections it is tempting to speculate that secretion of dsRNA was established as a disposal
393 mechanism by HCV allowing persistent replication in the same hepatocyte.

394 In summary, we report a novel immune escape mechanism employed by HCV to decrease the
395 activation of TLR3 in HCV-infected cells by secreting dsRNA. This mechanism underlines the
396 importance of TLR3-dependent responses in the course of HCV infection and might contribute to the
397 establishment and maintenance of chronic HCV infections.

398 **ACKNOWLEDGMENTS**

399 The authors thank Rahel Klein, Ulrike Herian, Uta Haselmann and Jutta Mohr for excellent technical
400 assistance and Vibor Laketa for microscopy support. We are grateful to the Electron Microscopy
401 Core Facility of the University of Heidelberg for providing access to their equipment and thanks to
402 Dr. Charlotta Funaya and Dr. Stefan Hillmer for technical support in EM work. A plasmid encoding
403 TLR3 was a kind gift from T. Espevik, NTNU, Trondheim, Norway. In addition, we thank Daniel
404 Lamarre for helpful discussions.

405

406 **REFERENCES**

- 407 1. Hajarizadeh B, Grebely J & Dore GJ Epidemiology and natural history of HCV infection. *Nat*
408 *Rev Gastroenterol Hepatol* 2013;10:553-562.
- 409 2. Romero-Brey I, Merz A, Chiramel A et al. Three-dimensional architecture and biogenesis of
410 membrane structures associated with hepatitis C virus replication. *PLoS Pathog*
411 2012;8:e1003056.
- 412 3. Wang H, Tai AW Continuous de novo generation of spatially segregated hepatitis C virus
413 replication organelles revealed by pulse-chase imaging. *J Hepatol* 2017;66:55-66.
- 414 4. Shulla A, Randall G Spatiotemporal analysis of hepatitis C virus infection. *PLoS Pathog*
415 2015;11:e1004758.
- 416 5. Hiet MS, Bauhofer O, Zayas M et al. Control of temporal activation of hepatitis C virus-
417 induced interferon response by domain 2 of nonstructural protein 5A. *J Hepatol*
418 2015;63:829-837.
- 419 6. Li K, Li NL, Wei D et al. Activation of chemokine and inflammatory cytokine response in
420 hepatitis C virus-infected hepatocytes depends on Toll-like receptor 3 sensing of hepatitis C
421 virus double-stranded RNA intermediates. *Hepatology* 2012;55:666-675.
- 422 7. Meylan E, Curran J, Hofmann K et al. Cardif is an adaptor protein in the RIG-I antiviral
423 pathway and is targeted by hepatitis C virus. *Nature* 2005;437:1167-1172.

- 424 8. Li K, Foy E, Ferreon JC et al. Immune evasion by hepatitis C virus NS3/4A protease-mediated
425 cleavage of the Toll-like receptor 3 adaptor protein TRIF. *Proc Natl Acad Sci U S A*
426 2005;102:2992-2997.
- 427 9. Jouan L, Melancon P, Rodrigue-Gervais IG et al. Distinct antiviral signaling pathways in
428 primary human hepatocytes and their differential disruption by HCV NS3 protease. *J Hepatol*
429 2010;52:167-175.
- 430 10. Dreux M, Garaigorta U, Boyd B et al. Short-range exosomal transfer of viral RNA from
431 infected cells to plasmacytoid dendritic cells triggers innate immunity. *Cell Host Microbe*
432 2012;12:558-570.
- 433 11. Bukong TN, Momen-Heravi F, Kodys K et al. Exosomes from hepatitis C infected patients
434 transmit HCV infection and contain replication competent viral RNA in complex with Ago2-
435 miR122-HSP90. *PLoS Pathog* 2014;10:e1004424.
- 436 12. Piper RC, Katzmann DJ Biogenesis and function of multivesicular bodies. *Annu Rev Cell Dev*
437 *Biol* 2007;23:519-547.
- 438 13. Luzio JP, Parkinson MD, Gray SR et al. The delivery of endocytosed cargo to lysosomes.
439 *Biochem Soc Trans* 2009;37:1019-1021.
- 440 14. Kowal J, Tkach M & Thery C Biogenesis and secretion of exosomes. *Curr Opin Cell Biol*
441 2014;29:116-125.
- 442 15. Elgner F, Ren H, Medvedev R et al. The Intracellular Cholesterol Transport Inhibitor U18666A
443 Inhibits the Exosome-Dependent Release of Mature Hepatitis C Virus. *J Virol* 2016;90:11181-
444 11196.
- 445 16. Shrivastava S, Devhare P, Sujjantararat N et al. Knockdown of Autophagy Inhibits Infectious
446 Hepatitis C Virus Release by the Exosomal Pathway. *J Virol* 2015;90:1387-1396.
- 447 17. Ramakrishnaiah V, Thumann C, Fofana I et al. Exosome-mediated transmission of hepatitis C
448 virus between human hepatoma Huh7.5 cells. *Proc Natl Acad Sci U S A* 2013;110:13109-
449 13113.
- 450 18. Koutsoudakis G, Herrmann E, Kallis S et al. The level of CD81 cell surface expression is a key
451 determinant for productive entry of hepatitis C virus into host cells. *J Virol* 2007;81:588-598.
- 452 19. Grunvogel O, Esser-Nobis K, Reustle A et al. DDX60L Is an Interferon-Stimulated Gene
453 Product Restricting Hepatitis C Virus Replication in Cell Culture. *J Virol* 2015;89:10548-10568.
- 454 20. Esser-Nobis K, Harak C, Schult P et al. Novel perspectives for hepatitis A virus therapy
455 revealed by comparative analysis of hepatitis C virus and hepatitis A virus RNA replication.
456 *Hepatology* 2015;62:397-408.
- 457 21. Belouzard S, Danneels A, Feneant L et al. Entry and release of hepatitis C virus in polarized
458 human hepatocytes. *J Virol* 2017.
- 459 22. Krieger SE, Zeisel MB, Davis C et al. Inhibition of hepatitis C virus infection by anti-claudin-1
460 antibodies is mediated by neutralization of E2-CD81-claudin-1 associations. *Hepatology*
461 2010;51:1144-1157.

- 462 23. Kleine M, Riemer M, Krech T et al. Explanted diseased livers - a possible source of metabolic
463 competent primary human hepatocytes. *PLoS One* 2014;9:e101386.
- 464 24. Klepper A, Eng FJ, Doyle EH et al. Hepatitis C virus double-stranded RNA is the predominant
465 form in human liver and in interferon-treated cells. *Hepatology* 2017;66:357-370.
- 466 25. Metz P, Dazert E, Ruggieri A et al. Identification of type I and type II interferon-induced
467 effectors controlling hepatitis C virus replication. *Hepatology* 2012;56:2082-2093.
- 468 26. Eyre NS, Aloia AL, Joyce MA et al. Sensitive luminescent reporter viruses reveal appreciable
469 release of hepatitis C virus NS5A protein into the extracellular environment. *Virology*
470 2017;507:20-31.
- 471 27. Kosaka N, Iguchi H, Yoshioka Y et al. Secretory mechanisms and intercellular transfer of
472 microRNAs in living cells. *J Biol Chem* 2010;285:17442-17452.
- 473 28. Ostrowski M, Carmo NB, Krumeich S et al. Rab27a and Rab27b control different steps of the
474 exosome secretion pathway. *Nat Cell Biol* 2010;12:19-30.
- 475 29. Dansako H, Yamane D, Welsch C et al. Class A scavenger receptor 1 (MSR1) restricts hepatitis
476 C virus replication by mediating toll-like receptor 3 recognition of viral RNAs produced in
477 neighboring cells. *PLoS Pathog* 2013;9:e1003345.
- 478 30. Grabski E, Wappler I, Pfaender S et al. Efficient virus assembly, but not infectivity,
479 determines the magnitude of hepatitis C virus-induced interferon alpha responses of
480 plasmacytoid dendritic cells. *J Virol* 2015;89:3200-3208.
- 481 31. Barouch-Bentov R, Neveu G, Xiao F et al. Hepatitis C Virus Proteins Interact with the
482 Endosomal Sorting Complex Required for Transport (ESCRT) Machinery via Ubiquitination To
483 Facilitate Viral Envelopment. *MBio* 2016;7.
- 484 32. Fahmy AM, Labonte P The autophagy elongation complex (ATG5-12/16L1) positively
485 regulates HCV replication and is required for wild-type membranous web formation. *Sci Rep*
486 2017;7:40351.
- 487 33. Boldanova T, Suslov A, Heim MH et al. Transcriptional response to hepatitis C virus infection
488 and interferon-alpha treatment in the human liver. *EMBO Mol Med* 2017;9:816-834.
- 489 34. Sheahan T, Imanaka N, Marukian S et al. Interferon lambda alleles predict innate antiviral
490 immune responses and hepatitis C virus permissiveness. *Cell Host Microbe* 2014;15:190-202.
- 491 35. Thomas E, Gonzalez VD, Li Q et al. HCV infection induces a unique hepatic innate immune
492 response associated with robust production of type III interferons. *Gastroenterology*
493 2012;142:978-988.
- 494 36. Serti E, Werner JM, Chattergoon M et al. Monocytes activate natural killer cells via
495 inflammasome-induced interleukin 18 in response to hepatitis C virus replication.
496 *Gastroenterology* 2014;147:209-220.
- 497 37. Kloss V, Grunvogel O, Wabnitz G et al. Interaction and Mutual Activation of Different Innate
498 Immune Cells Is Necessary to Kill and Clear Hepatitis C Virus-Infected Cells. *Front Immunol*
499 2017;8:1238.

- 500 38. Wieland S, Makowska Z, Campana B et al. Simultaneous detection of hepatitis C virus and
501 interferon stimulated gene expression in infected human liver. *Hepatology* 2014;59:2121-
502 2130.
- 503 39. Kandathil AJ, Graw F, Quinn J et al. Use of laser capture microdissection to map hepatitis C
504 virus-positive hepatocytes in human liver. *Gastroenterology* 2013;145:1404-1413.
- 505 40. Haruna Y, Kanda T, Honda M et al. Detection of hepatitis C virus in the bile and bile duct
506 epithelial cells of hepatitis C virus-infected patients. *Hepatology* 2001;33:977-980.
- 507 41. Heidrich B, Steinmann E, Plumeier I et al. Frequent detection of HCV RNA and HCVcoreAg in
508 stool of patients with chronic hepatitis C. *J Clin Virol* 2016;80:1-7.
509
510
511 Author names in bold designate shared co-first authorship.

512

513 **FIGURE LEGENDS**

514 **Figure 1: Strand-specific detection of HCV RNA in cells and EVs**

515 (A) Schematic of the HCV genome used for infection (upper) and the subgenomic replicon used to
516 select stable cell lines (lower). HCVcc was derived from the genotype 2a (chimera Jc1), while
517 subgenomic replicons were of genotype 1b (isolate Con1) and genotype 2a (isolate JFH-1). (B) Huh7-
518 Lunet-CD81^{high} cells were infected with HCVcc at MOI = 0.1. After 72h, HCV positive and negative
519 strand RNA was quantified in intracellular (i.c.) RNA and RNA from EVs by strand-specific RT-qPCR.
520 Bars represent mean values with range from independent experiments (n=2). (C) Huh7-Lunet-
521 CD81^{high} cells were infected with HCVcc at MOI = 0.1. At the respective time points, positive and
522 negative strand RNA was quantified in EVs isolated from infected cells by strand-specific RT-qPCR.
523 Shown are mean values with range from independent experiments (n=2). (D) PHH were infected
524 with HCVcc at MOI = 0.1. At the respective time points, positive and negative strand RNA was
525 quantified in EVs isolated from infected cells by strand-specific RT-qPCR. Shown are mean values
526 with range from two wells of one representative donor. (E) HCV positive and negative strand RNA
527 was quantified in i.c. RNA and RNA from EVs isolated from HCV-infected PHH 72h after infection by
528 strand-specific RT-qPCR. Bars represent mean values with SD from 3 independent donors (n=3). (F),

529 (G) HCV positive and negative strand RNA was quantified in i.c. RNA and RNA from EVs isolated from
530 HCV replicon cells (F: genotype 1b, isolate Con1; G: genotype 2a, isolate JFH-1) by strand-specific RT-
531 qPCR. Bars represent mean values with SD from independent experiments (n=3). (H) The data from
532 (B), (E), (F), and (G) was used to calculate the ratio of negative to positive HCV strands. Bars
533 represent mean values with SD. Statistical significance was assessed by Welch's test.

534 **Figure 2: Detection of HCV replication complexes in the late endosomal compartment**

535 (A) Schematic of HCV NS5A-mCherry reporter replicon RNA used for CLEM. (B),(C) Huh7-Lunet cells
536 were electroporated with replicon RNA and 72 hours after electroporation, CLEM was performed to
537 correlate the NS5A-mCherry signal with the ultrastructure detected by EM. Scale bar represents 200
538 nm. Asterisks indicate DMVs. Areas in (C) were chosen to display the most commonly observed
539 NS5A positive ultrastructural features, DMVs (area 2) and MVB with DMV (area 3, 4). (D) NS5A-
540 positive areas were scored for correlation with cellular structures. LD: lipid droplet. Bars represent
541 mean values with SD of 5 cells from 2 different dishes. (E) NS5A-mCherry-positive MVB/lysosomes or
542 unmarked MVB/lysosomes from the same cells were scored for their content. If a DMV or MMV was
543 present in the structure, it was scored as positive. Bars represent mean values with SD of 5 cells
544 from 2 independent experiments. Statistical significance was assessed by paired t test. (F), (G) HCV
545 subgenomic replicon cell lines were stained with antibodies against dsRNA (J2) and late endosomal
546 markers. Scale bar represents 5 μ m. (H) Percentage of dsRNA signal colocalizing with late endosomal
547 markers was determined after 3D reconstruction of HCV replicon cells. 8 cells from two independent
548 experiments were analyzed. Error Bars represent SD.

549 **Figure 3: Impact of EV release block on dsRNA levels**

550 HCV replicon cell lines were transfected with siRNA against Rab27a, or left untreated. 40 hours after
551 transfection, untreated cells were treated with 1 μ M Bafilomycin A (BafA). 8h later, EVs were
552 isolated from the supernatants, and cells were processed for immunofluorescence and microscopy.
553 (A) HCV RNA copies in EVs were detected by RT-qPCR. Bars represent mean values with SD from

554 independent experiments (n=4). (B) HCV RNA copies in EVs were detected by RT-qPCR. Bars
555 represent mean values with SD from independent experiments (n=3). (C) dsRNA in Rab27a-
556 transfected cells was detected by IF staining for dsRNA. 10 cells were analyzed from 2 independent
557 experiments. . (D) dsRNA in BafA-treated cells was detected by IF staining for dsRNA. 11 cells were
558 analyzed from 2 independent experiments. (E, G) dsRNA colocalized with CD63 (E) or Lamp1 (G) was
559 detected in siRab27a- or siNT transfected cells by IF staining and confocal microscopy. At least 11
560 cells were analyzed from 2 independent experiments. (F, H) dsRNA colocalized with CD63 (F) or
561 Lamp1 (H) was detected in BafA-treated or control cells by IF staining and confocal microscopy. At
562 least 11 cells were analyzed from 2 independent experiments. Statistical significance was assessed
563 by Welch's test.

564 **Figure 4: Activation of TLR3 by HCV replication**

565 (A) Huh7-Lunet cells overexpressing PRRs and PHH were transfected with 100 ng/well poly(I:C) or
566 stimulated with 50 µg/ml poly(I:C) in the supernatant (SN) for endosomal delivery. 8h after
567 stimulation, total RNA was isolated and IFIT1 mRNA levels were quantified by RT-qPCR as readout
568 for PRR activation. Bars represent mean values with SD from technical triplicates from one
569 experiment (n=1). (B) Schematic representation of HCV luciferase reporter replicons. (C) Huh7-Lunet
570 cells stably transduced with respective PRRs were electroporated with HCV luciferase reporter
571 replicon RNA. At the respective timepoints, RNA was isolated and IFIT1 mRNA was quantified by RT-
572 qPCR. Values shown are mean values with SD from independent experiments (n=3). HCV replication
573 was monitored in parallel by luciferase assay. (D) HCV replication in Huh7-Lunet empty/RIG-
574 I/MDA5/TLR3 cells was determined by luciferase assay. Mean values with SD from independent
575 experiments are shown (n=3). (E) Schematic representation of selectable HCV reporter replicons. (F),
576 (G) HCV reporter replicon cell lines were transduced with lentiviruses coding for TLR3 or a control
577 vector at MOI = 5. 48 hours after transduction, IFIT1 mRNA was measured by RT-qPCR to determine
578 TLR3 activation and luciferase assay was performed to determine replication of HCV. (F) IFIT1 mRNA
579 levels. Bars represent mean values with range from independent experiments (n=2). (G) HCV

580 replication was determined by luciferase assay. Bars represent mean values with SD from
581 independent experiments (n=3). (H) Huh7-Lunet-empty or -TLR3 cell lines were electroporated with
582 HCV reporter replicon RNA and co-cultured with mock-electroporated Huh7-Lunet-TLR3 or -empty
583 cells, respectively. 72h after electroporation, RT-qPCR was performed to determine IFIT1 mRNA
584 levels. Values were normalized a co-culture of mock-electroporated Huh7-Lunet-empty and -TLR3
585 cells. Bars represent mean values with SD from independent experiments (n=4). Statistical
586 significance was assessed by Welch's test.

587 **Figure 5: Impact of EV release on TLR3 activation**

588 (A),(B),(C),(D) Huh7-Lunet-empty or -TLR3 cell lines were electroporated with HCV reporter replicon
589 RNA and indicated siRNAs. 4h after electroporation, cells were treated with 10 μ M GW4869 or
590 DMSO. At the indicated timepoints, total RNA was isolated and IFIT1 mRNA was quantified by RT-
591 qPCR. HCV replication was monitored by luciferase activity. Small panels below the graphs show
592 blow-ups of IFIT1 mRNA levels at 48h ((A),(B)) or luciferase activity at 96h after electroporation
593 ((C),(D)). (A) IFIT1 mRNA levels in Huh7-Lunet-empty cells. (B) IFIT1 mRNA levels in Huh7-Lunet-TLR3
594 cells. (C) HCV replication as determined by luciferase assay in Huh7-Lunet-empty cells. (D) HCV
595 replication as determined by luciferase assay in Huh7-Lunet-TLR3 cells. (E), (F) Huh7-Lunet-
596 CD81^{high}-empty or -TLR3 cells were transfected with siRNAs against Rab27a or a control siRNA. 16
597 hours after transfection, cells were infected with HCVcc at MOI=5. 6h after infection, treatment with
598 GW4869 or DMSO was started. At the indicated timepoints, total RNA was isolated and IFIT1 mRNA
599 was quantified by RT-qPCR. IFIT1 mRNA levels of empty cells are shown in (E), IFIT1 mRNA levels of
600 TLR3 cells are shown in (F). All values shown are mean values with SD from independent
601 experiments (n=3 for A,B,C,D; n=2 for E,F). Statistical significance was assessed by Welch's test.

602 **Figure 6: Polarized secretion of HCV RNA**

603 HepG2-based cell clones Clone 15 and 1SC3 were polarized on transwell dishes and infected with
604 HCVcc. 48 hours after infection, RNA was isolated from apical and basolateral supernatants. (A,C)

605 HCV positive and negative strand RNA was detected by strand-specific RT-qPCR in supernatants from
606 Clone 15 and Clone 1SC3, respectively. (B,D) Ratio of negative to positive stand HCV RNA in
607 supernatants from Clone 15 and Clone 1SC3, respectively. All bars represent mean values with SD
608 from independent experiments (n=3 for Clone 15, n=2 for clone 1SC3). (E) EVs were isolated from 1
609 ml of serum from chronic HCV patients, and used for strand-specific RT-qPCR for HCV RNA. Shown
610 are mean values of technical triplicates with SD from each donor. Numbers indicate ratios between
611 positive and negative strand HCV RNA. Statistical significance was assessed by Welch's test.

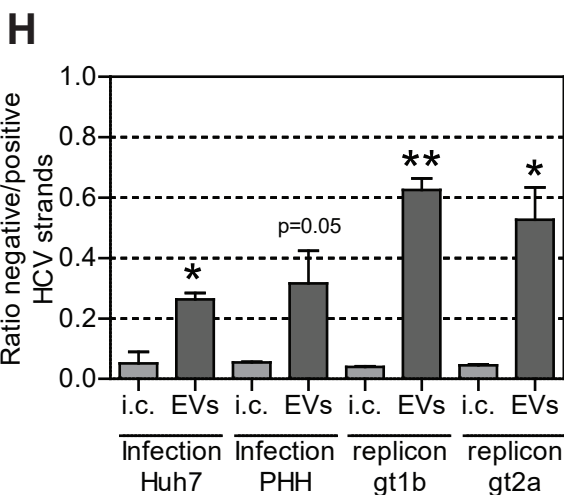
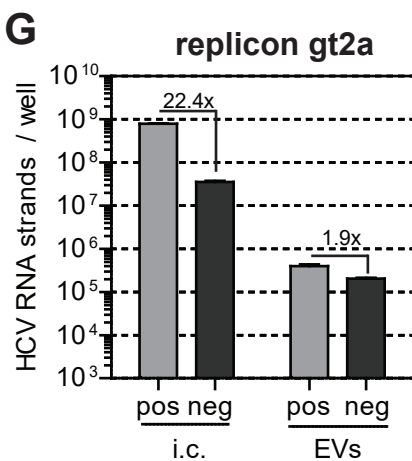
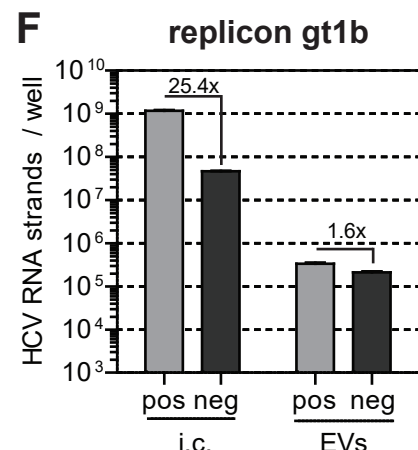
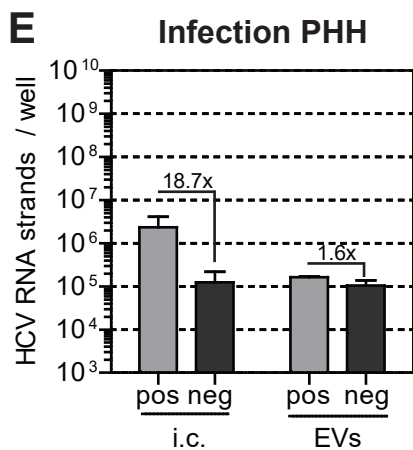
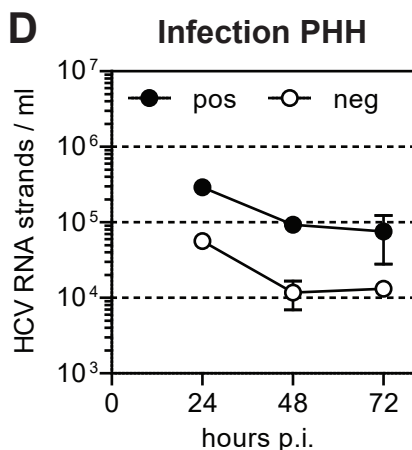
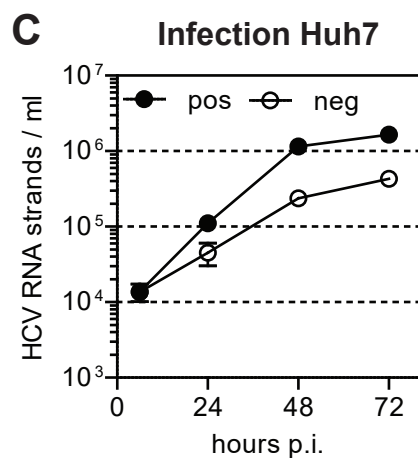
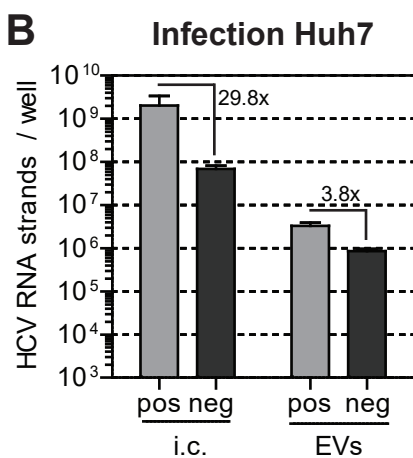
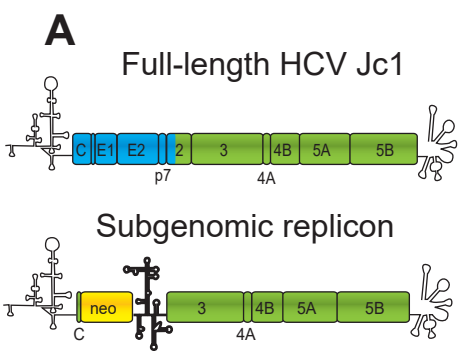
612 **Figure 7: Model of novel immune attenuation mechanism.**

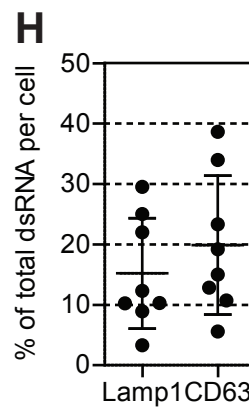
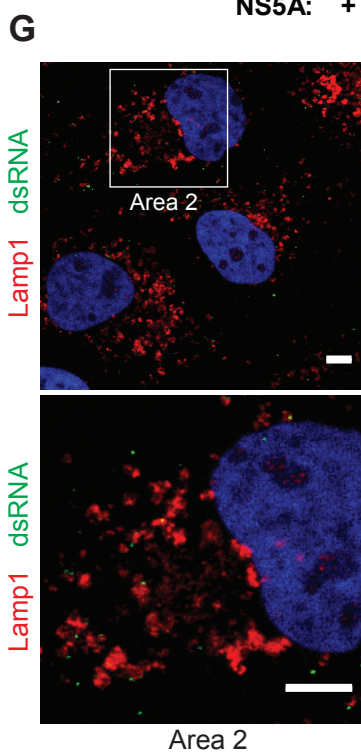
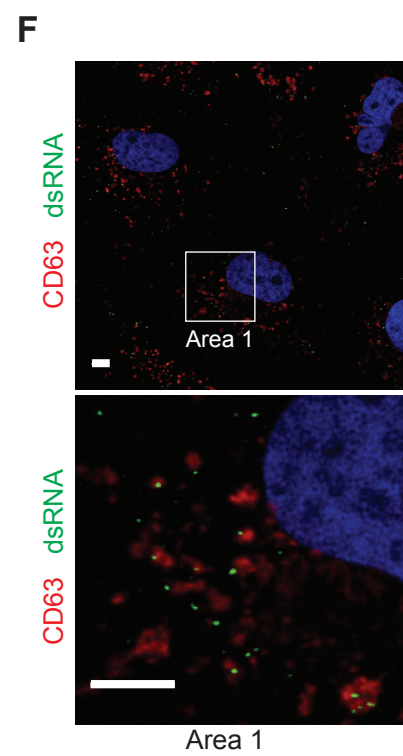
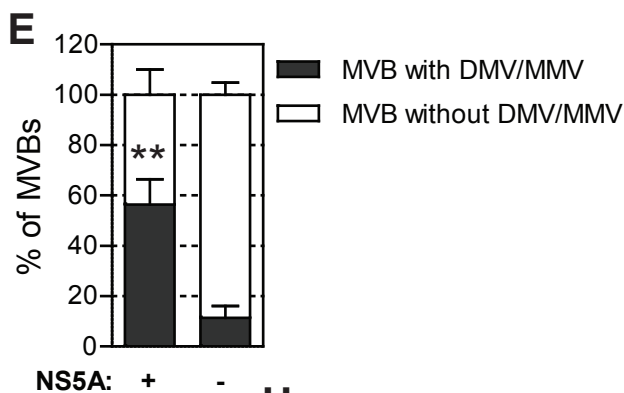
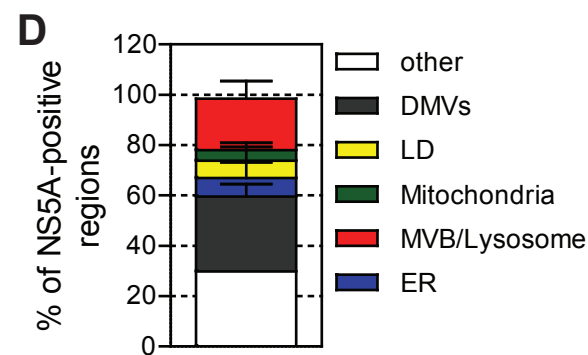
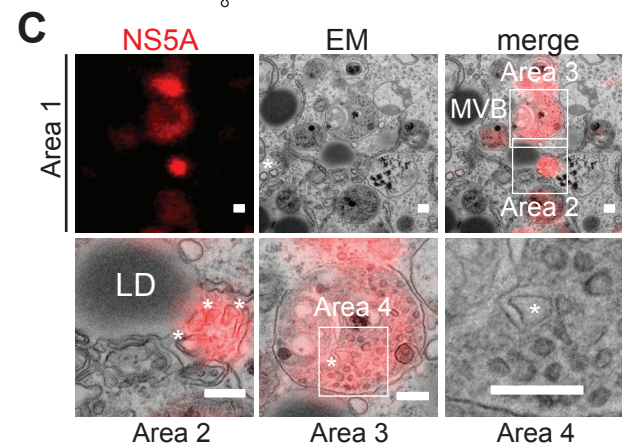
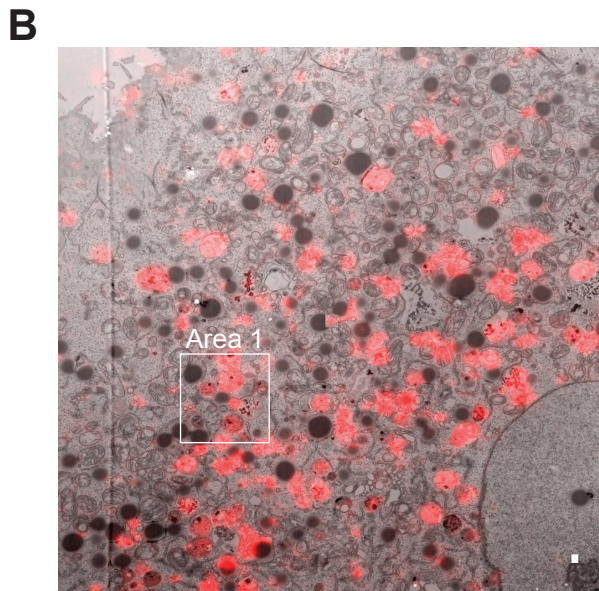
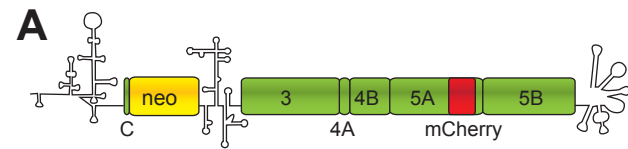
613 (A) HCV dsRNA from the replication complexes is transported to the LE/MVB. From there, it can be
614 degraded in the lysosome, secreted at the apical or basolateral compartments in EVs or activate
615 TLR3 in the late endosome, inducing the induction antiviral ISGs that inhibit HCV replication. (B)
616 Blocking of EV release results in increased dsRNA levels, enhancing TLR3 activation. This leads to a
617 stronger production of antiviral ISGs, and a stronger inhibition of HCV replication.

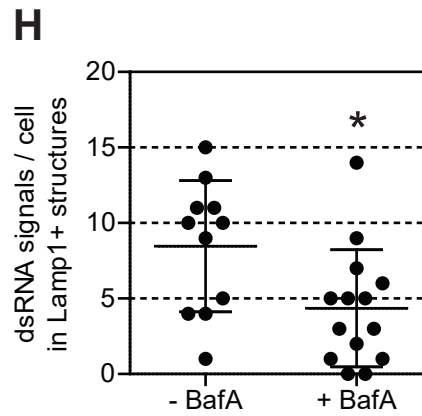
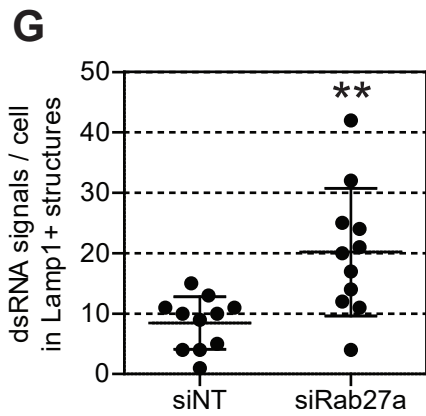
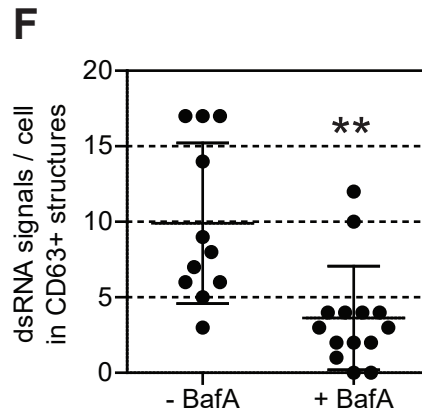
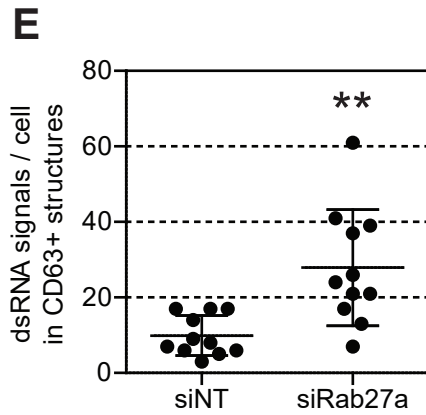
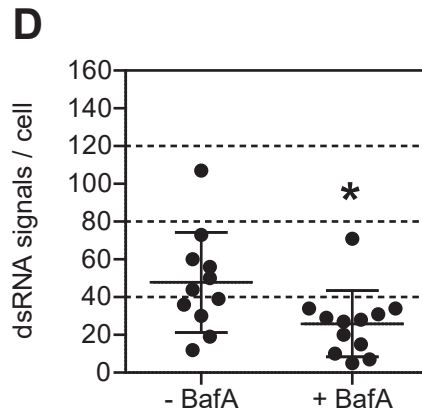
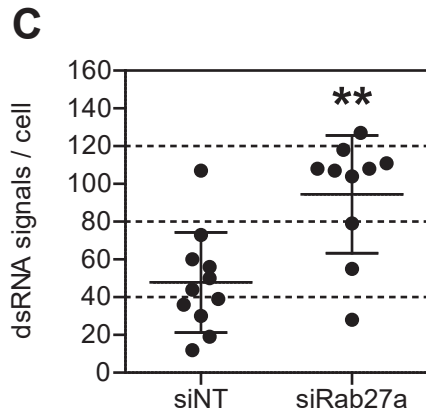
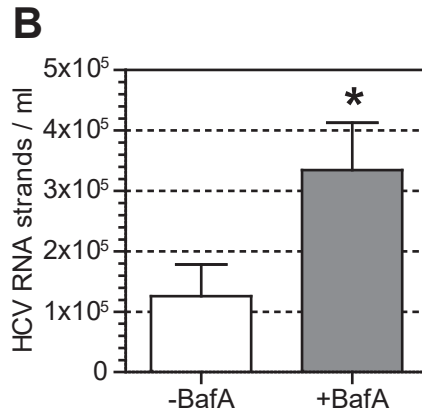
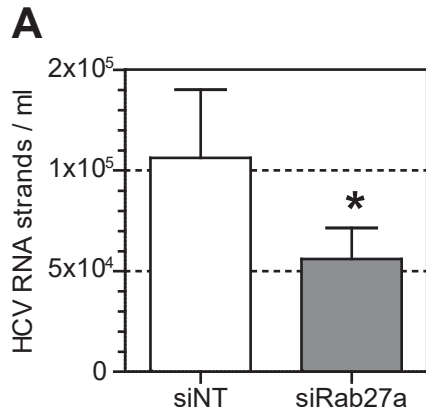
618

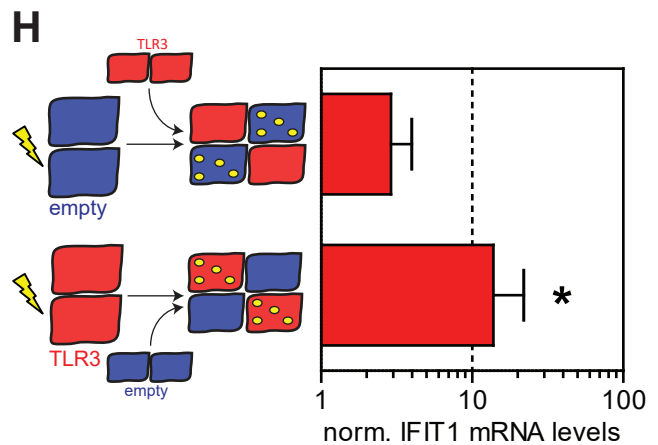
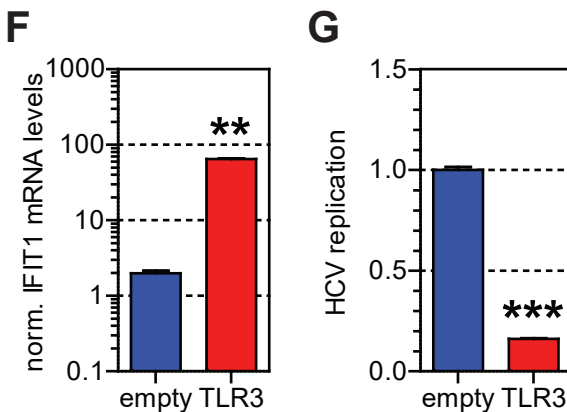
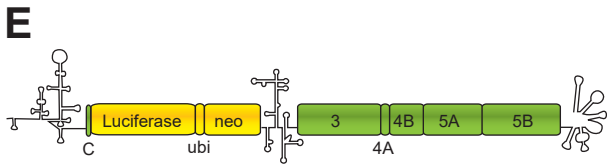
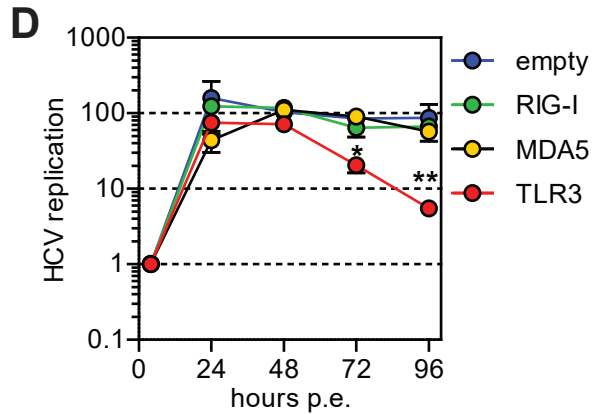
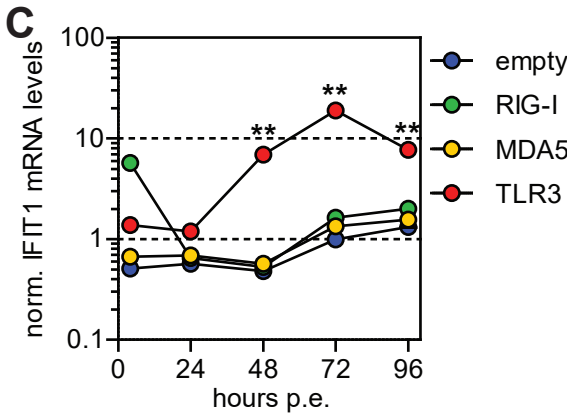
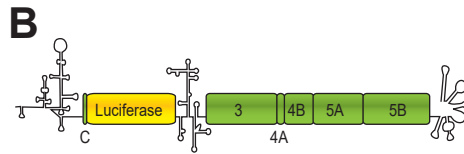
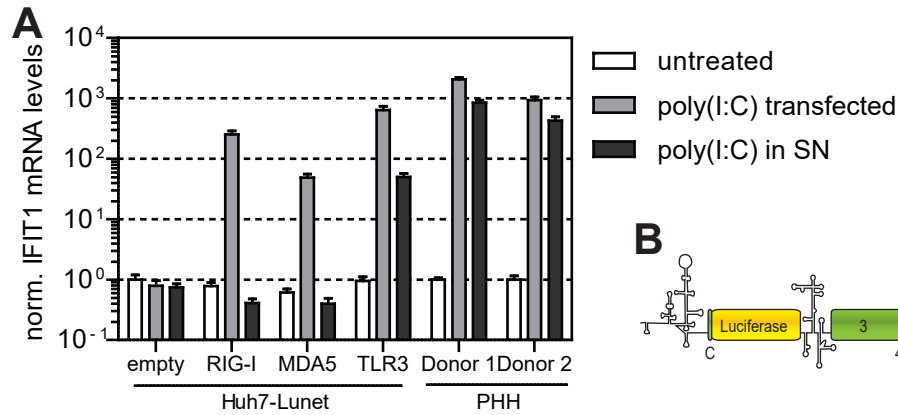
619

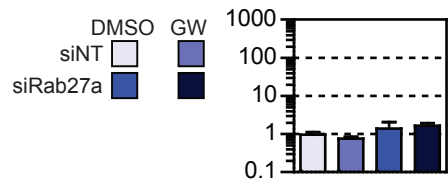
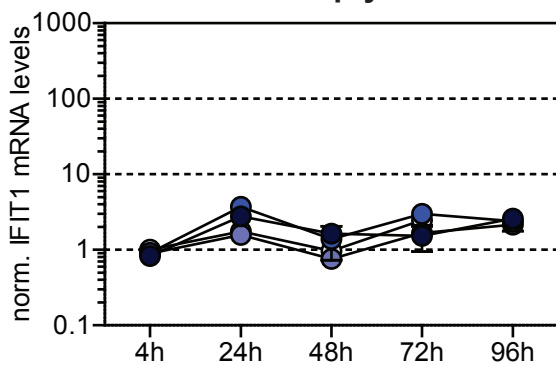
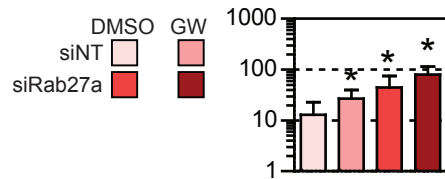
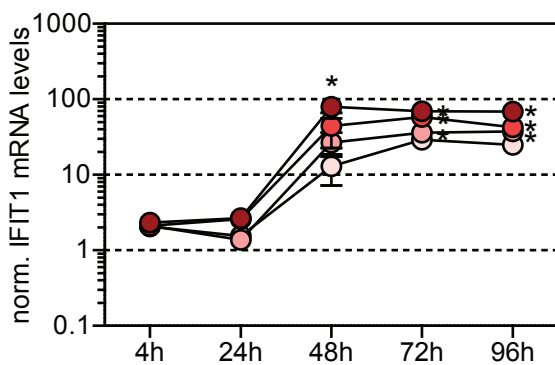
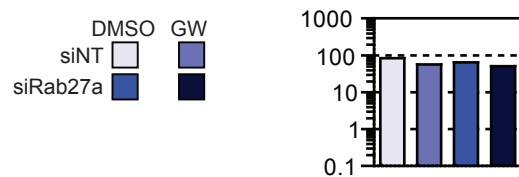
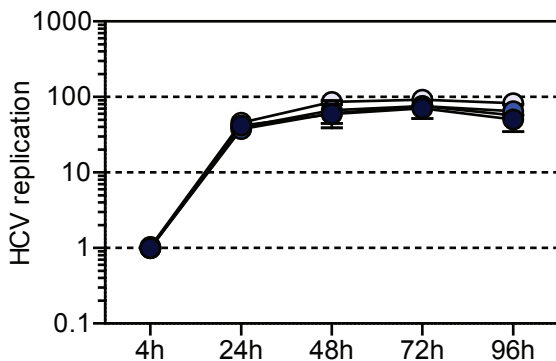
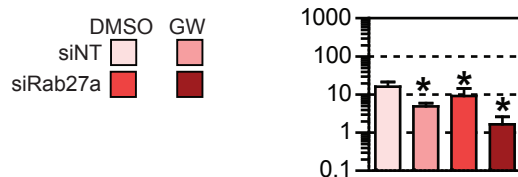
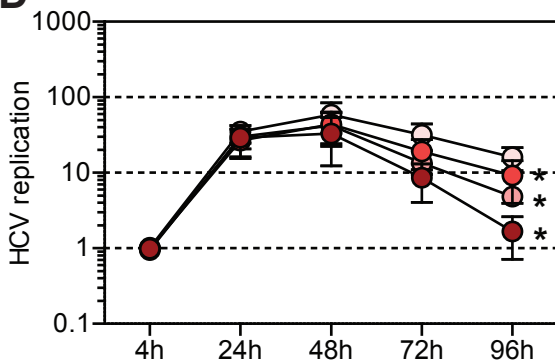
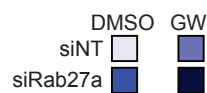
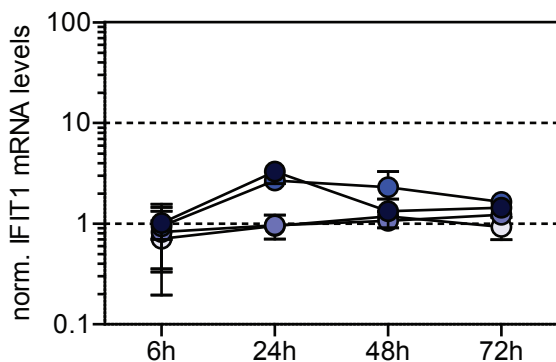
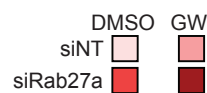
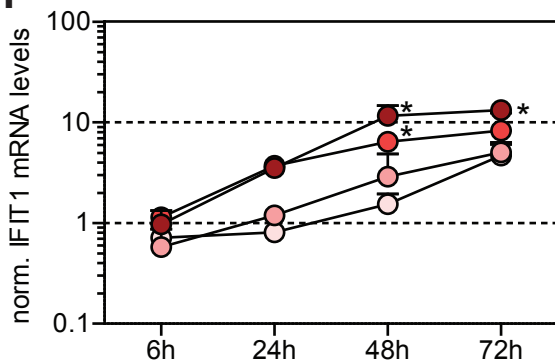
620

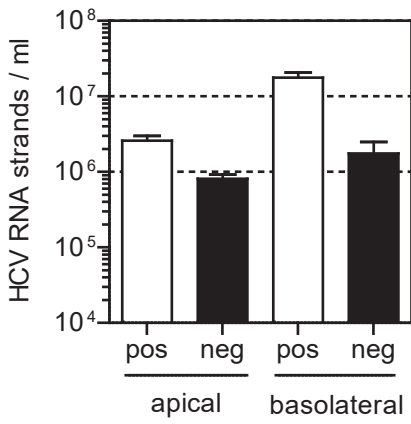
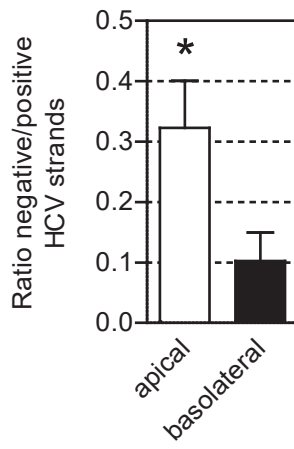
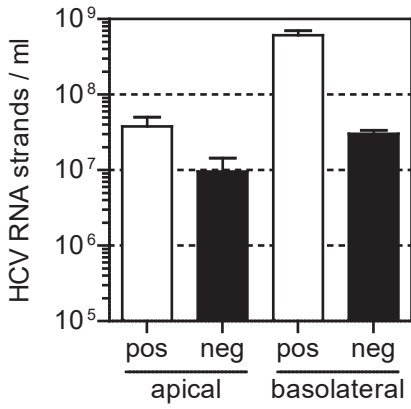
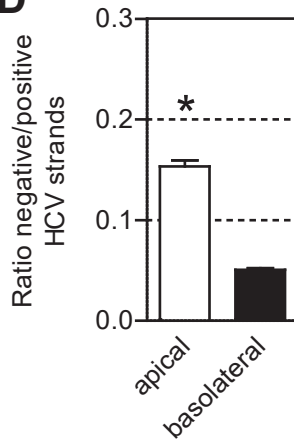
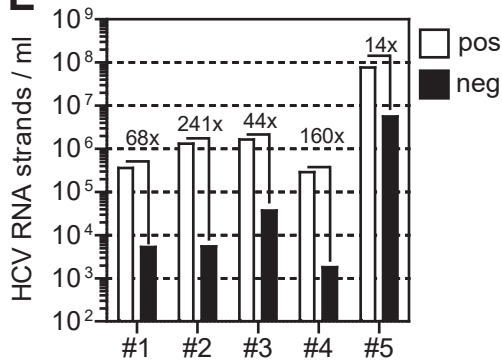


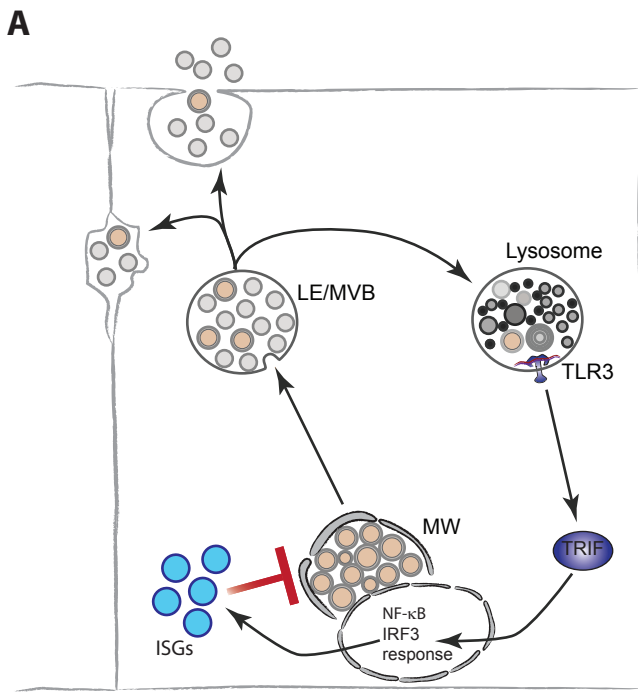




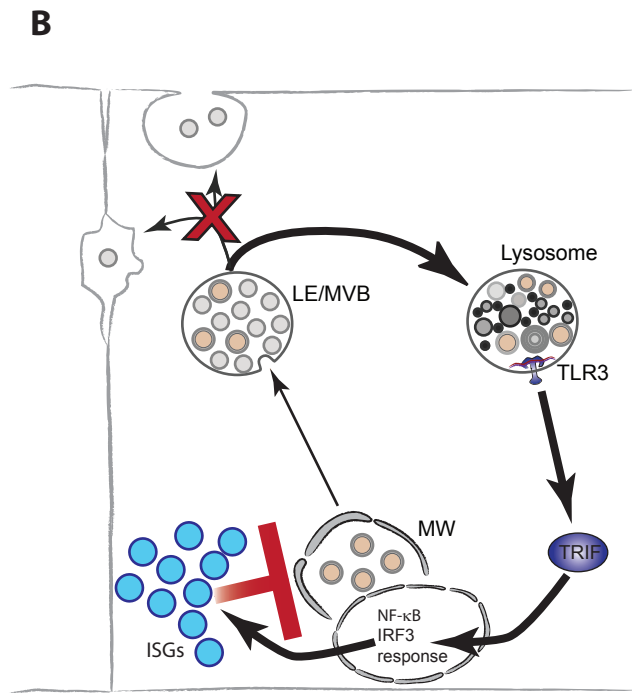


A**empty****replicon****B****TLR3****replicon****C****replicon****D****replicon****E****infection****F****infection**

A**Clone 15****B****C****Clone 15C3****D****E**



Normal state



EV release blocked